ejpmr, 2021,8(8), 587-596.

SJIF Impact Factor 6.222

EUROPEAN JOURNAL OF PHARMACEUTICAL AND MEDICAL RESEARCH

www.ejpmr.com

Research Article

ISSN 2394-3211

EJPMR

NEW SULFONYL PYRIMIDINES INDUCE APOPTOSIS THROUGH DNA CLEAVAGE PATHWAY

Priyanka Yadav[1], Shafia Mir[1], Praveen Kumar[1] and Ayaz Mahmood Dar[*2]

[1]Department of Chemistry OPJS University 331001 Rajasthan.
[2]Department of Chemistry Govt. Degree College Sogam 193223 Kashmir.

***Corresponding Author: Ayaz Mahmood Dar**

Department of Chemistry Govt. Degree College Sogam 193223 Kashmir.

Article Received on 10/06/2021 **Article Revised on 30/06/2021** **Article Accepted on 20/07/2021**

ABSTRACT

The new sulfonyl pyrimidinones (**4-6**) were synthesized by the reaction of sulfonyl thiosemicarbazones (**1-3**) with ethyl cyanoacetate in absolute ethanol. After characterization by spectral and analytical data, the DNA interactions of the compounds were carried out by UV-vis, fluorescence spectroscopy, circular dichroism, molecular docking and gel electrophoresis. The compound binds to DNA preferentially through electrostatic interactions with K_b; 2.93 $\times 10^3$ M^{-1}, 3.03 $\times$ 10^3 M^{-1} and 3.11 $\times$ 10^3 M^{-1}, respectively depicting the higher propensity of compound **6** with CT DNA. Gel electrophoresis depicted that compound **6** brought conversion of SC form (Form II) into LC form (Form III) of DNA at 4.0 μM. The docking study suggested that the intercalation of compounds in between the nucleotide base pairs is due to the pyrimidinone moiety of the sulfone derivative. The circular dichroism studies suggest that compounds (**4-6**) affect the helicity of B-DNA. During *in vitro* cytotoxicity, compound (**4-6**) revealed potential toxicity against the different human cancer cells. AO/EB staining analysis clearly indicates that compound **5** causes apoptosis in cancer cells. The results revealed that compound **5** has better prospectus to act as a cancer chemotherapeutic candidate, which warrants further *in vivo* anticancer investigations.

KEYWORDS: Sulfonyl pyrimidinones, Thiosemicarbazones, DNA binding, MTT.

1. INTRODUCTION

DNA is a polyelectrolyte with a high negative charge. It has a double stranded structure due to hydrogen bonds, π-π and hydrophobic interactions between nitrogen base pairs. The electrostatic interactions of cations located on the nucleic acid surface with DNA phosphates provide stability to the structure.[1] Although the most stable conformation under physiological conditions is the B-DNA form, the adopted conformation depends on the presence in the medium of various agents such as alcohol[2], heterocyclic compounds[3], multivalent ions[4], positively charged polypeptides[5], histones[6], polyamines[7] and nanoparticles.[8] Physico-chemical parameters such as salt concentration, solvent dielectric constant or temperature also induce conformational changes in the biomacromolecule.[9]

In molecular biology and drug development, the cleaving agents of DNA have attracted extensive attention due to their potential applications.[10] The phosphodiester bonds of DNA are extremely stable and the half life of DNA for hydrolysis is estimated to be around 200 million years under uncatalyzed physiological conditions.[11] Metal complexes have been widely investigated as cleaving agents of nucleic acids and are found to be reasonably efficient[12], but their use in pharmacy is restricted because of serious issues over the lability and toxicity produced due to free radical generation of some transition metals during the redox processes.[13] To overcome these limitations of toxicity, Gobel and co-workers[14] put forward the concept of 'metal-free cleaving agents' which are being applied to active phosphodiesters like 'nucleic acid mimics' and RNA.

The literature reveals that a large number of heterocyclic derivatives have shown potential binding to DNA. In most of the intercalation complexes, the substituted pyrimidinone derivatives are located in either of the grooves with pyrimidinone chromophore sandwiched between base pairs. The ability of these intercalators to direct functionality into either of the grooves of nucleic acids makes them good candidates for selective ligands which are able to provide molecular recognition.[15] The planar pyrimidinone scaffold of one of the sulfonyl pyrimidine derivatives also acted as a potent fluorescent ligand intercalating between DNA base pairs and showed the potential anticancer activity. In addition to this, the pyrimidines further more showed the apoptotic degradation of DNA.[16] Metal free heterocyclic compounds are also able to inhibit topoisomerase I and II enzymes, disrupt DNA repair and replication, and induce cell death without showing toxicity towards the normal cells.[17,18] The cytotoxicity of most metal free heterocyclic based drugs are based on their ability to

suppress topoisomerase activity[19] hence the topoisomerase acts as an endogenous poison and may induce apoptosis.[20]

In continuation of our previous work[21], herein, we report the synthesis of new sulfonyl pyrimidinones as metal free DNA binding agents. The synthesized compounds were characterized by elemental analysis and spectral techniques including IR, ^{1}H NMR, ^{13}C NMR and MS. The UV-vis absorption, fluorescence, gel electrophoresis and molecular docking studies were employed to study the binding pattern and interaction of these compounds with DNA while as MTT Assay and confocal microscopy was employed to study the cytotoxicity of the these compounds and morphological changes in cancer cells, respectively.

2. EXPERIMENTAL

All the melting points were determined on a Kofler apparatus and are uncorrected. The IR spectra were recorded on KBr pellets with Perkin Elmer RXI Spectrophotometer and values are given in cm^{-1}. ^{1}H and ^{13}C NMR spectra were run in CDCl3 on a JEOL Eclipse (400 MHz) instrument with TMS as internal standard and values are given in ppm (δ). Mass spectra were recorded on a JEOL SX 102/DA-6000 Mass Spectrometer. Thin layer chromatography (TLC) plates were coated with silica gel G and exposed to iodine vapours to check the homogeneity as well as the progress of reaction. Petroleum ether refers to a fraction of boiling point 60-80 °C. Sodium sulfate (anhydrous) was used as a drying agent. All the chemicals were purchased from Merck India and were used after distillation. Super coiled pBR322 DNA was purchased from GeNei (India) while as double-stranded calf thymus DNA, purchased from Sigma, was dissolved in a 0.1 M Tris-buffer. The purity of DNA was verified by monitoring the ratio of absorbance at 260 nm to that at 280 nm, which was in the range 1.8-1.9. The DNA concentration was spectrophotometrically determined using ϵ_{260} = 6600 M^{-1} cm^{-1}.[22] The human cancer cell lines used for the cytotoxicity experiment were MCF-7, HeLa, HL-60, SW480 and HepG2 which were obtained from the National Cancer Institute (NCI), biological testing branch, Frederick Research and Development Centre, USA.

General Synthesis of novel sulfonyl pyrimidinones (4-6)

To a solution of compounds (**1-3**)[23] (1.5 mmol), in absolute ethanol (20 mL), an equimolar amount of ethyl cyanoacetate was added. The reaction mixture was refluxed for 5 h. The progress and completion of the reaction was monitored by TLC. After completion of the reaction, the excess solvent was removed to three fourths of the original volume under reduced pressure. The reaction mixture was then taken in diethyl ether, washed with water and dried over anhydrous sodium sulphate. Evaporation of solvents and recrystallization from acetone afforded respective products (**4-6**).

6-Amino-1-[2-benzenesulfonyl-1-(4-nitro-phenyl)-ethylideneamino]-2-thioxo-2,3-dihydro-1H-pyrimidin-4-one (***4***)

Off white crystals, m.p. 151 °C, IR (KBr, cm^{-1}): 3335 (NH), 1665 (*CO*NH), 1640 (C=N), 1235 (C=S), 1020 (C-N), 1620 (C=C arom), S=O (1400), N=O (1510); ^{1}H NMR ($CDCl_3$) δ: 8.14-7.72 (m, 4H, arom.), 7.61-7.15 (m, 5H, arom.), 6.8 (s, 1H, N*H*, exchangeable with D_2O), 4.77 (s, 2H), 2.0 (s, 2H, NH_2, exchangeable with D_2O), 5.38 (s, 1H, C_5'-H). ^{13}C NMR ($CDCl_3$), δ: 181 (C=S), 169 (C=O), 160.8 (C=N), 131 (C_5'), 111 (C_6'), 124.0 (2CH), 128.5 (2CH), 129.4 (2CH), 130.5 (2CH), 134.6 (2CH), 138.4 (C), 140.0 (C), 64.0 (CH_2). Anal. Calcd for $C_{18}H_{15}N_5O_5S_2$: C, 48.53, H, 3.39, N, 15.72 found: C, 48.42, H, 3.17, N, 15.67; ESI MS: *m/z* 445 [M$^{+\cdot}$].

6-Amino-1-[1-(4-nitro-phenyl)-2-(toluene-4-sulonyl)-ethylideneamino]-2-thioxo-2,3-dihydro -1H-pyrimidin-4-one (***5***)

Yellow crystals, m.p. 166 °C, IR (KBr, cm^{-1}): 3335 (NH), 1665 (*CO*NH), 1640 (C=N), 1235 (C=S), 1020 (C-N), 1620 (C=C arom), S=O (1400), N=O (1510); ^{1}H NMR ($CDCl_3$), δ: 8.22-7.81 (m, 4H, arom.), 7.72-7.40 (m, 4H, arom.), 7.3 (s, 1H, NH, exchangeable with D_2O), 4.34 (s, 2H), 2.47 (s, 3H), 2.2 (s, 2H, NH_2, exchangeable with D_2O), 5.31 (s, 1H, C_5'-H). ^{13}C NMR ($CDCl_3$), δ: 184 (C=S), 164 (C=O), 157.5 (C=N), 21.7 (CH_3), 64.2 (CH_2), 131 (C_5'), 111 (C_6'), 124.0 (2CH), 128.5 (2CH), 130.0 (2CH), 130.5 (2CH), 135.4 (2C), 140.0 (C), 145.9 (C), 107 (C-N). Anal. Calcd for $C_{19}H_{17}N_5O_5S_2$: C, 49.66, H, 3.73, N, 15.24 found: C, 49.55, H, 3.47, N, 14.97; ESI MS: *m/z* 459 [M$^{+\cdot}$].

6-Amino-1-[2-(4-nitro-benzenesulfonyl)-1-(4-nitrophenyl)-ethylideneamino]-2-thioxo-2,3-dihydro-1H-pyrimidin-4-one (***6***)

White crystals, m.p. 146 °C, IR (KBr, cm^{-1}): 3335 (NH), 1665 (*CO*NH), 1640 (C=N), 1235 (C=S), 1020 (C-N), 1620 (C=C arom), S=O (1400), N=O (1510); ^{1}H NMR ($CDCl_3$) δ: 8.11-7.77 (m, 4H, arom.), 7.62-7.40 (m, 4H, arom.), 7.33 (s, 1H, NH, exchangeable with D_2O), 4.84 (s, 2H), 2.4 (s, 2H, NH_2, exchangeable with D_2O), 5.20 (s, 1H, C_5'-H). ^{13}C NMR ($CDCl_3$), δ: 181.5 (C=S), 164 (C=O), 162 (C=N), 124.2 (2CH), 124.5 (2CH), 130.3 (2CH), 130.4 (2CH), 139.5 (2C), 143.6 (2C), 100 (C_2'-N), 131 (C_5'), 97 (C_6'-N), 63.4 (CH_2). Anal. Calcd for $C_{18}H_{14}N_6O_7S_2$: C, 44.08; H, 2.88; N, 17.13. Found: C, 43.91; H, 2.71; N, 17.01. ESI MS: *m/z* 490 [M$^{+\cdot}$].

DNA binding studies

Absorption and Emission Spectroscopy

The DNA binding experiments were carried out by using absorption titration and emission spectroscopy as per the practices reported in literature.[24] The UV-vis spectra for DNA compound (**4-6**) interactions were obtained using an Agilent 8453 spectrophotometer while as fluorescence measurements were carried out with a JASCO spectrofluorimeter (FP 6200). Solutions of DNA and compound (**4-6**) were scanned in a 1 cm quartz cuvette. To eliminate the absorbance of the DNA while

measuring the absorption spectra, an equal amount of DNA was added to both the compound solution and the reference solution.

DNA cleavage experiments

Cleavage experiments were performed with Axygen agarose electrophoresis[25] connected to a Genei 50-500 V power supply, visualized and photographed by the Vilber-INFINITY gel documentation system. Cleavage experiments of supercoiled pBR322 DNA (300 ng) by compound **6** (1.0-5.0 μM) in a 5mM Tris-HCl/50mM NaCl buffer at pH 7.2 were carried out and the reaction followed by agarose gel electrophoresis. The samples were incubated for 1 h at 37 °C. A loading buffer, containing 25% bromophenol blue, 0.25% xylene cyanol and 30% glycerol, was added and electrophoresis was carried out at 60 V for 1 h in a Tris-HCl buffer using a 1% agarose gel containing 1.0 mg/mL of ethidium bromide.

Circular dichroism

CD spectra of CT DNA (200 mM) were analysed in the absence and presence of increasing concentration of compounds. Spectra were run for R values 5, 2.5, 1.6 and 1.25 ($R^{¼}$ [DNA]/[compound]). CD spectra were taken as the average of three independent scans between 220 and 330 nm using JASCO J-815CD spectrometer with 150 W Xenon arc lamp.

Molecular docking

The rigid molecular docking studies were performed using HEX 6.1 software.[26] The initial structure of the compound **6** was generated by Mercury modeling software. The molecules of compound **6** were optimized for use in the following docking study. The crystal structure of the B–DNA dodecamer $d(CGCAAATTTCGC)_2$ (PDB ID: 1BNA) was downloaded from the Protein Data Bank. All calculations were carried out on an Intel CORE i5, 2.6 GHz based machine running MS Windows 7 as the operating system. Visualization of the docked pose has been done using Discovery Studio graphics programs.

In vitro cytotoxicity

MTT Assay

To study the cytotoxic effect of the compounds **4-6**, *in vitro* MTT assay was carried out.[27] Human cancer cell lines **SW480** (colon adenocarcinoma cells)/ATCC (CCL-228), **HeLa** (cervical cancer cells)/ATCC (CCL-2), **MCF-7** (breast cancer cells)/ATCC (HTB-22), **HepG2** (hepatic carcinoma cells)/ATCC (CRL-8065) and **HL-60** (Leukaemia cells)/ATCC (CCL-240) were taken for the study. SW480, HL-60 and HepG2 cells were grown in RPMI 1640 supplemented with 10% foetal bovine serum (FBS), 10U penicillin and 100μg/mL streptomycin at 37 °C with 5% CO_2 in a humidified atmosphere. HeLa and MCF7 cells were grown in Dulbecco's modified Eagle's medium (DMEM) supplanted with FCS and antibiotics as described above for RPMI 1640. The cells were incubated in an incubator at 37 °C and 5% CO_2. After 24 h, the cells were serum starved overnight and compounds **4-6** were then added prepared in DMSO in a concentration range of 3-100 μM, ensuring an equal volume of 200 μL across the wells of the plate. The plate was further incubated at 37 °C and 5% CO_2 for 48 h. The cytotoxicity of the compounds was tested by the addition of the yellow tetrazolium salt MTT (3-(4, 5-dimethylthiazolyl-2)-2,5-diphenyltetrazolium bromide) prepared in culture medium at a working concentration of 0.4 mg/mL across the plate. The plate was further incubated for 2 h so that the MTT is reduced by the live cells, to produce a purple Formazan product. After this time, the medium was aspirated and 200 μL of DMSO (Sigma Ltd.) was added to each well. The experiment was performed in triplicates. The plate was agitated gently for 5 min. before measuring the optical density at 570 nm in each well using Thermo Scientific multi-plate reader (MultiSkan EX Elisa reader). Since the absorbance correlated with the number of viable cells the percentage of viability was calculated from the absorbance. The IC_{50} values of the compounds were determined by plotting the percentage viability versus concentration on a logarithmic graph and the reading of the concentration at which 50% of cells are viable relative to the control.

AO/EB staining

Apoptotic morphology was studied by staining the cells with a combination of the fluorescent DNA-binding dyes AO and EB. Cells were harvested and washed three times with phosphate-buffered saline (PBS) after being incubated with different concentrations of compound **6** for 72 h, and then was stained with 5 μg/mL AO and EB (AO/EB; Sigma) for 3 min, then washed three times with PBS. Apoptotic morphology of the different cell types were observed under a fluorescence microscope (Leica, German).

3. RESULTS AND DISCUSSION

Chemistry

Development of highly functional molecules from simple building blocks has always attracted the curiosity of synthetic chemists. So we herein report synthesis of new sulfonyl pyrimidinones from sulfonyl thiosemicarbazones & ethyl cyanoacetate under reflux; on the completion of the reaction, the products were obtained in better yields (70-80%).

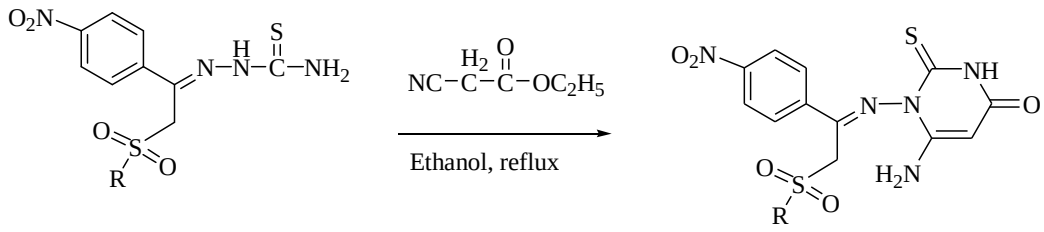

(**1-3**)

(**4-6**)

R	**R**
(**1**) C_6H_5-	(**4**) C_6H_5-
(**2**) *p*-CH_3-C_6H_4-	(**5**) *p*-CH_3-C_6H_4-
(**3**) *p*-NO_2-C_6H_4-	(**6**) *p*-NO_2-C_6H_4-

Scheme 1. Pathway for the formation of sulfonyl pyrimidines 4-6

The mechanism for the formation of compounds **4-6** involves the nucleophilic attack of the nitrogen of thiosemicarbazone on the carbonyl carbon of ethyl cyanoacetate, making the ethoxy group to leave, with a simultaneous attack of another thiosemicarbazone nitrogen on the cyano group of ethyl cyanoacetate, converting it to =C–NH_2, which leads to the formation of a pyrimidine heterocyclic moiety appended with a sulfone skeleton.

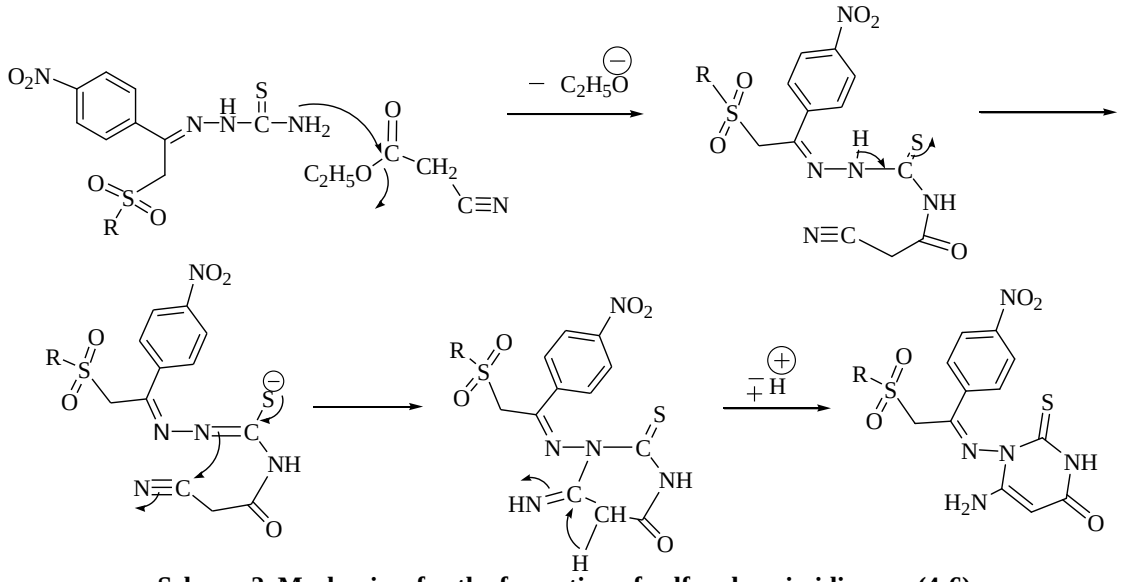

Scheme 2. Mechanism for the formation of sulfonyl pyrimidinones (4-6)

The characterization studies are in good agreement with the proposed structures for sulfonyl pyrimidinones **4-6** shown in **Scheme 1**. In the IR spectra, the absorption bands in the ranges 3353 and 3290 cm^{-1} were attributed to the NH, NH2 groups, respectively, while a strong absorption band at 1665cm^{-1} confirmed the presence of the CONH group in compounds **4-6**. In our ^1H NMR study, the two singlets in the range δ 7.3-6.8 and 2.0-2.4 confirmed the presence of NH and NH_2, respectively, while the singlet at δ 5.2-5.38 depicted the presence of an olefinic proton in compounds **4-6**. In our ^{13}C NMR study, the signals at δ 181-184.5, 164-169, 157-162, 130-131.4 confirmed the presence of the C=S, C=O, C=N, C=C groups, respectively, in compounds **4-6**. Finally, the presence of distinct molecular ion peaks [$M^{+\cdot}$] at m/z 445, 459 and 490 in the MS spectra also proved the formation of the compounds **4-6**. This strategy can also be applied to diverse thiosemicarbazones; in that way pyrimidinones may also allow further modifications on the substituted heterocyclic systems.

DNA Binding

Electronic absorption titration

The UV-vis spectra of compounds (**4-6**) exhibited intense absorption bands at 260 nm attributed to the π→π* or intraligand transitions as shown in **Fig. 1**. This intense ligand (π→π*) absorption band is used to monitor the interaction of the compounds with calf thymus DNA. Upon the addition of increasing concentration of DNA (0.70×10^{-5} − 4.24×10^{-5} M) to the test compounds in 2% DMSO/5mM Tris HCl/50mM NaCl buffer solution, there was an increase in the absorption intensity of the intraligand absorption band 'hyperchromism' without shift in position of the band. Hyperchromicity and hypochromicity are the spectral features of DNA concerning its double helical structure. The hyperchromic effect reflects the corresponding

changes of DNA in its conformation and structure and results from the structural damage to the secondary structure DNA double helix.[28] These spectral characteristics suggested that compounds exhibited higher binding propensity with DNA and interacts presumably by minor groove interaction *via* the phosphate backbone of DNA double helix together with the hydrophobic interaction. The hydrophobic interaction with DNA replaces the water molecules in the DNA grooves leading to the enhancement in entropy and stabilization of the DNA–bound compound.[29]

In order to further compare the binding strength of the compounds, their intrinsic binding constant (K_b) were determined from the following equation (1).[30]

$$[DNA]/|\varepsilon_a - \varepsilon_f| = [DNA]/|\varepsilon_b - \varepsilon_f| + 1/K_b|\varepsilon_b - \varepsilon_f| \quad (1)$$

Where, [DNA] represents the concentration of DNA, ε_a, ε_f and ε_b are the apparent extinction coefficients A_{obs}/[M], the extinction coefficient for free compound and the extinction coefficient for compound in the fully bound form, respectively. In the plots of [DNA] / ε_a–ε_f versus [DNA], K_b is given by the ratio of the slope to the intercept.

The intrinsic binding constants for compounds (**4-6**) were found to be 2.93 ×10^3 M^{-1}, 3.03 × 10^3 M^{-1} and 3.11 × 10^3 M^{-1} respectively. The results obtained revealed that compound **6** binds more strongly with CT DNA as compared to the remaining compounds and the binding affinity follows the order **6**>**5**>**4**. Interestingly, the intrinsic binding K_b value of compound **6** is higher in magnitude which may be due to the presence of additional interaction or bonding due to NO_2 group with DNA base pair.

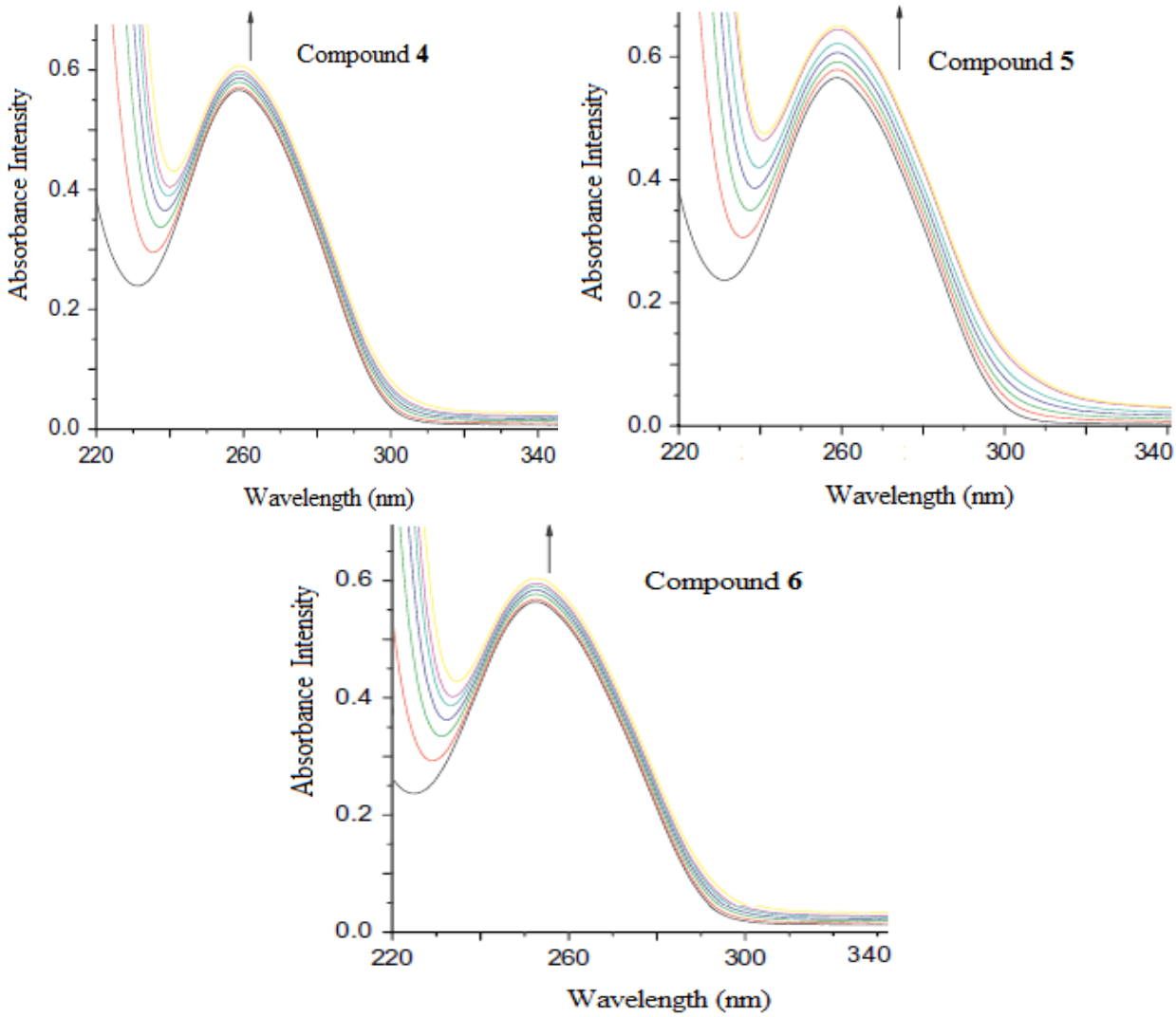

Fig. 1. UV-vis absorption spectra show the variation of for compounds (4-6) with increase in the concentration of CT DNA. The arrow shows the change in intensity with increasing DNA concentration.

Fluorescence spectroscopy

The emission spectra of compound (**4-6**) displayed intense luminescence at 600 nm at room temperature in the absence of DNA when excited at 350 nm. On addition of increasing concentration of DNA (0.70 × 10^{-5} to 4.24 × 10^{-5} M) to the fixed amount of compounds (1 ×

10^{-4} M), the emission intensity appreciably increase as shown in **Fig. 2**. The increase in the emission intensity is largely due to the change in environment around compounds and related to the extent to which the molecule is inserted into the hydrophobic environment of DNA minor and major grooves. Since DNA is a hydrophobic molecule it reduces the accessibility of solvent molecules to reach the hydrophobic environment inside the DNA helix, and the mobility of the compound is restricted at the binding site ultimately leading to decrease in vibrational mode of relaxation.[31] Furthermore, the binding of compound to the DNA helix could decrease the collisional frequency of solvent molecules with the compound, leading to the change in the emission of compound. These results revealed that interaction between CT DNA and compound occurs due to the hydrophobicity of both molecules.

To compare the binding affinity of compounds to DNA quantitatively, the binding constant '**K**' and binding site number '**n**' were calculated by using Scatchard equation (2) and (3).[32]

$$\mathbf{C_F = C_T\,(F/F_o - P)\,(1 - P)} \quad (2)$$

$$\mathbf{r/c = K\,(n - r)} \quad (3)$$

Where, C_F is the concentration of free compound, C_T is the total concentration of compound; F and F_o are fluorescence intensities in the presence and absence of DNA, respectively. P is the ratio of observed fluorescence quantum yield of the bound compound to that of the free compound. The value P was obtained as the intercept by extrapolating from a plot of F/F_o versus 1/[DNA], r denotes the ratio of $C_B = (C_T – C_F)$ to the DNA concentration, 'c' is the free compound concentration and 'n' is the binding site number.

The binding constants for compounds (**4-6**) were calculated to be 2.2×10^3 M^{-1}, 2.7×10^3 M^{-1} and 3.3×10^3 M^{-1}, respectively. The number of binding sites 'n' for compounds (**4-6**) were found to be 1.04, 1.13 and 1.52, respectively indicating that compound **6** has higher DNA binding propensity in agreement with the electronic absorption titration experiment.

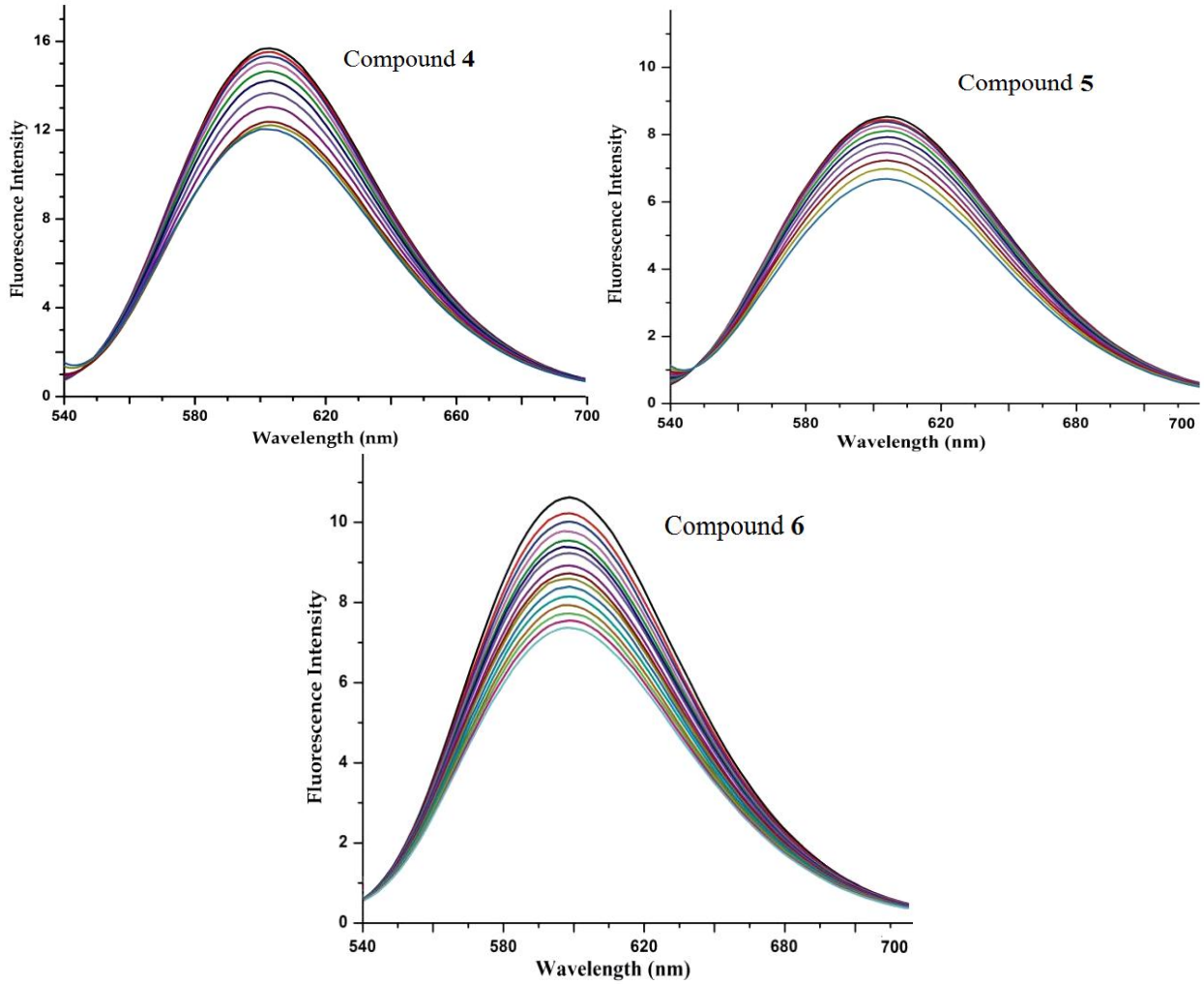

Fig 2. Fluorescence titration of given compounds (4-6) with the CT DNA. Fluorescence intensity increases with subsequent addition of DNA solution.

DNA cleavage/nuclease activity

The DNA cleavage was controlled by the relaxation of supercoiled circular form of pBR322 DNA into the nicked and linear form. When a circular plasmid DNA is subjected to agarose gel electrophoresis, the fastest migration will be observed for supercoiled form (Form I). If one strand is cleaved, the supercoil will relax to produce a slower moving open circular form (Form II). If both strands are cleaved, a linear form (Form III) will be generated that migrates in between Form I and Form II. The DNA cleaving ability of compound **6** was investigated using pBR322 DNA. In the absence of any external additives the compound **6** cleaved double stranded supercoiled plasmid DNA (SC form: Form I) (300 ng) in 5mMTris-HCl/50mMNaCl buffer into nicked circular form (NC form: Form II) after 1 h of incubation at physiological pH 7.2 and temperature 25 °C. Keeping the DNA concentration constant (300 ng) the concentration of compound **6** was varied (1.0-6.0 μM) and the cleavage reaction was further monitored by gel electrophoresis. The results revealed concentration-dependent electrophoretic cleavage i.e. at 2.0 μM concentration showing the conversion of SC form (Form I) to NC form (Form II). At 4.0 μM concentration, compound **6** exhibited efficient nuclease activity i.e. conversion of SC form (Form II) into LC form (Form III). Presence of Form I, and II of pBR322 DNA indicated that compound **6** is involved in double strand DNA cleavage (**Fig. 3**).

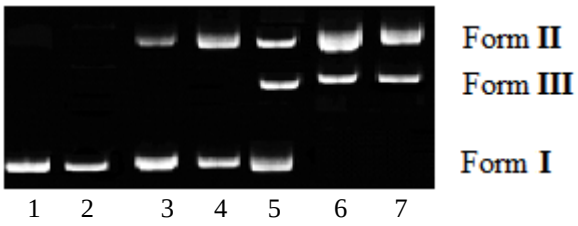

Fig. 3. Agarose gel electrophoresis patterns of pBR322 plasmid DNA (300 ng) cleaved by compound 6 (1.0-6.0 μM), after 1 h incubation time (concentration dependent) Lane 1: Control; Lane 2: 1.0 μM 6 + DNA; Lane 3: 2.0 μM 6 + DNA; Lane 4: 3.0 μM 6 + DNA. Lane 5: 4.0 μM 6 + DNA; Lane 6: 5.0 μM 6 + DNA; Lane 7: 6.0 μM 6 + DNA in buffer (5 mM Tris-HCl/50 mM NaCl, pH 7.2 at 25 °C)

Circular dichroism

The conformation and helicity changes of CT DNA in the presence of the compounds (**4-6**) were studied using circular dichroism and the results are shown in **Fig. 4**. Because of the base stacking a positive peak at 275 nm and due to helicity a negative peak at 245 nm was observed.[33] DNA was incubated for 30 min with different concentrations of the compounds (**4-6**) (r([DNA]/[Compound] = 5 to 1.25). Intensity of both the positive and negative band of DNA has been found to decrease in the presence of the compounds (**4-6**). However, the change in the intensity of the negative peak is more pronounced than the change in the positive peak intensity. This observation clearly shows that compounds (**4-6**) affect the helicity of B-DNA.

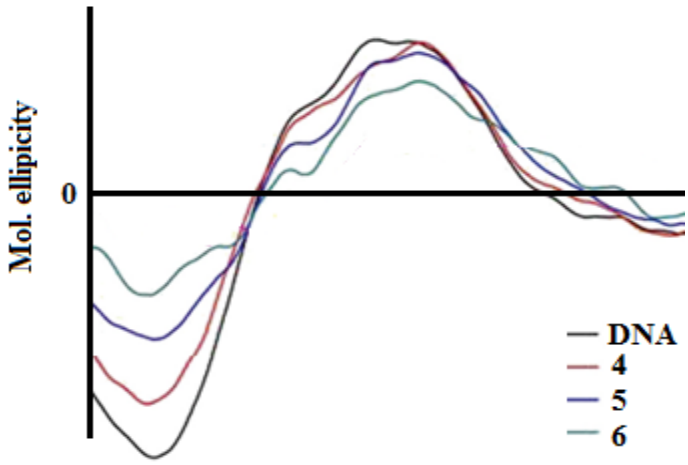

Fig. 4. CD spectra of CT DNA in the presence of different compounds (4-6)

In vitro cytotoxicity

The *in vitro* anticancer activity was measured using the MTT assay during which the conversion of the soluble yellowish MTT to the insoluble purple formazan by active mitochondrial lactate dehydrogenase of living cells has been used to develop an assay system for measurement of cell proliferation.[27] Since literature reveals that pyrimidine derivatives being similar to 5-Fluorouracil, a known anticancer drug (which is also pyrimidine derivative) which defines its potentially activeness against different cancer cells, hence with this intuition, a series of pyrimidinone derivatives were synthesized and subsequently *in vitro* anticancer activity was carried out.

Table 1. MTT assay showing the IC_{50} values by 4-6, Cisplatin and 5-Fu against given panel of cancer cell lines.

	IC_{50} (µM)				
Comp.	**Breast**	**Cervical**	**Leukemia**	**Colon**	**Hepatic**
	MCF-7	**HeLa**	**HL-60**	**SW480**	**HepG2**
4	11.35	16.81	14.27	21.01	**10.31**
5	**9.52**	19.13	11.53	17.32	21.52
6	10.36	10.55	8.26	10.04	19.51
5-FU	8.40	7.32	6.45	9.71	7.31
Cisplatin	6.23	5.21	5.83	4.62	5.78

5-FU = 5-Fluorouracil

During the screening, all the three pyrimidinone derivatives (**Table 1**) depicted potential cytotoxic behaviour by showing less inhibition count particularly compound **4** showed IC_{50} 11.35 µM and 10.31 µM against MCF-7 and HepG2 cell line, respectively. The compound **5** also revealed potential inhibition i.e. 9.52 µM against MCF-7 cell line. The inhibition depicted by compound **6** was 10.36 µM, 10.04 µM and 8.26 µM against MCF-7, HeLa and HL-60 cell lines, respectively. The planar and Π electron system in aromatic ring of the compound results in higher hydrophobicity which could deeply penetrate into the base pairs of DNA, thereby leading to higher DNA binding propensity. This in turn can lead the DNA damage which causes the growth inhibition of cancer cells.

Morphological examination (AO/EB staining)

MCF-7 cells were stained with Hoechst 33342-PI (propidium iodide) and AO (acridine orange)/EB (ethidium bromide). After MCF-7 cells were exposed to various concentrations of compounds for 72 h, different morphological features were shown. In AO/EB staining, uniformly, green live cells with normal morphology were seen in the control group (**Fig. 5**). Early apoptotic cells with nuclear condensation occurred. Orange later apoptotic cells with fragmented and apoptotic bodies were seen in compounds-treated groups.[34] In Hoechst/PI staining, control cells displayed normal growth characteristics with few dead cells. However, most nuclei with the treatment of **5** were condensed and densely stained with blue or pink fluorescence. The results suggest that cells in the treatment with compound **5** were apoptotic, whereas almost no apoptotic cell was detected in the control group.

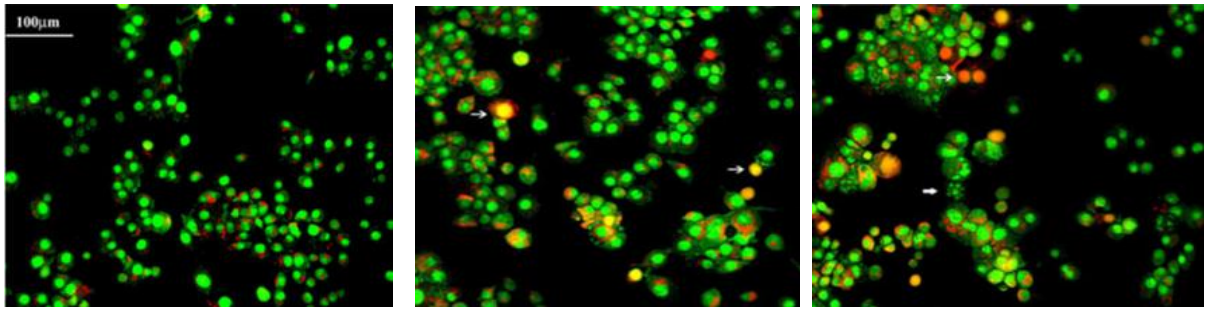

Control **5 µM Compound 5** **15 µM Compound 5**

Fig. 5. Apoptosis detections by AO/EB and Hoechst/PI staining on MCF-7 cells treated with different concentrations of compound 5 for 72 h.

Molecular docking

In our experiment, rigid molecular docking (two interacting molecules were treated as rigid bodies) studies were performed to predict the binding modes of compounds with a DNA duplex of sequence $d(CGCAAATTTCGC)_2$ dodecamer (PDB ID: 1BNA), and provided energetically favourable docked structure (DNA–compound complex shown in **Fig. 6**). Compound **6** is depicting electrostatic interaction with one hydrogen bond of binding energy of –275.27 kcal, and docking score of –6.1. It is evident from the figure that these types of compounds get attached with DNA through electrostatic as well as hydrophobic interactions.

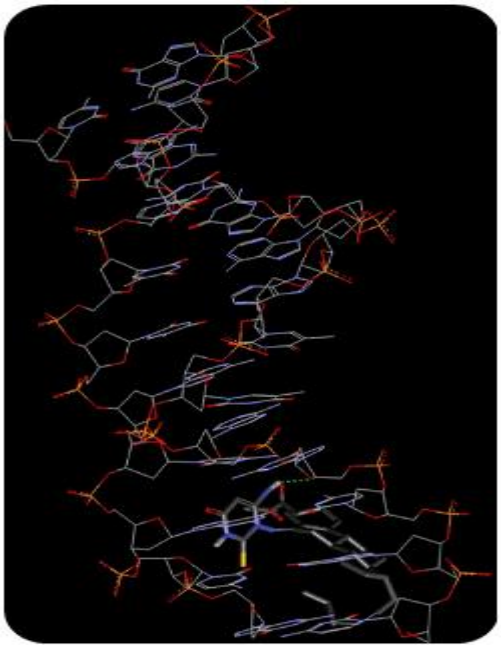

Fig. 6. Molecular docked model of compound 6 with DNA dodecamer duplex of sequenced $(CGCGAATTCGCG)_2$ (PDB ID: 1BNA) and the green dashed lines showing hydrogen bond interaction between them.

The sulfone moiety due to these stereochemical reasons remains far from the nucleotide base pairs, and hence it is the pyrimidinone moiety with groups like –NH, –CO and – NH_2 that shows an intercalation between the nucleotide base pairs of DNA through hydrogen bonding. Thus binding energy and docking score values are consistent with the high-binding constant obtained from spectroscopic values. Thus, we can conclude that there is a mutual complement between spectroscopic techniques and molecular modelling, which can provide valuable information about the mode of interaction of the compounds with DNA and the conformation constraints for adduct formation.

4. CONCLUSION

We successfully synthesized sulfonyl pyrimidinones from sulfonyl thiosemicarbazones. From spectroscopic titration, compounds bind to DNA (CT DNA) effectively through electrostatic and hydrophobic interactions. The absorption and fluorescence studies reveal the stabilization of the energy levels of the compounds in the presence of DNA. The DNA cleavage, CD spectra, and molecular modeling studies revealed the potential binding interaction capacity of these compounds with DNA molecule. From in vitro cytotoxicity screening, it is clear that sulfonyl pyrimidinones were found to be potential cytotoxic agents against the panel of cancer cell. Hence, the present study has shown that these synthesized sulfonyl pyrimidinones can be used as a template for future development through modification and derivatization to design more potent and selective cytotoxic and DNA-binding agents.

5. ACKNOWLEDGMENTS

The authors are thankful to the Department of Chemistry, OPJS University, for providing necessary financial and research facilities for the successful completion of the work.

REFERENCES

1. R.S. Dias, B. Lindman, DNA Interactions With Polymers and Surfactants, Wiley and Sons, New Jersey, 2008 2.
2. J.C. Girod, W.C.J. Johson, S.K. Huntington, M.F. Maestre, Conformation of deoxyribonucleic acid in alcohol solutions, Biochemistry, 1983; 12: 5092–5096.
3. X. Meng, L. Liu, C. Zhou, L. Wang, C. Liu, Dinuclear copper(II) complexes of a polybenzimidazole ligand: their structures and inductive roles in DNA condensation, Inorg. Chem., 2008; 47: 6572–6574.
4. R.W.Wilson, V.A. Bloomfield, Counterion-induced condensation of deoxyribonucleic acid. A light-scattering study, Biochemistry, 1979; 18: 2192–2196.
5. P. Cohen, C. Kidson, Conformational analysis of DNA-poly-L-lysine complexes by optical rotatory dispersion, J. Mol. Biol., 1968; 35: 241–245.
6. A.J. Adler, E.C. Moran, G.D. Fasman, Complexes of DNA with histones f2a2 and f3, Biochemistry, 1975; 14: 4179–4185.
7. L.C. Gosule, J.A. Schellamn, Compact form of DNA induced by spermidine, Nature, 1976; 259: 333–335.
8. A.A. Zinchenko, T. Sakaue, S. Aaraki, K. Yoshikawa, D. Baigl, Single-chain compaction of long duplex DNA by cationic nanoparticles: modes of interaction and comparison with chromatin, J. Phys. Chem. B, 2007; 111: 3019–3031.
9. A. Estévez-Torres, D. Baigl, DNA compaction: fundamentals and applications, Soft Matter, 2011; 7: 6746–6756.
10. R.M. Burger, Cleavage of nucleic acids by bleomycin, Chem. Rev., 1998; 98: 1153–1169.
11. D.S. Sigman, A. Mazumder, D.M. Perrin, Chemical nucleases, Chem. Rev., 1993; 93: 2295–2316.
12. Y. Jin, J.A. Cowan, DNA cleavage by copper-ATCUN complexes. Factors influencing cleavage mechanism and linearization of dsDNA, J. Am. Chem. Soc., 2005; 127: 8408–8415.
13. J. Smith, K. Ariga, E.V. Anslyn, Enhanced imidazole-catalyzed RNA cleavage induced by a bis-alkyl guanidinium receptor, J. Am. Chem. Soc., 1993; 115: 362–364.
14. U. Scheffer, A. Strick, V. Ludwig, S. Peter, E. Kalden, M.W. Gobel, Metal-free catalysts for the hydrolysis of RNA derived from guanidines, 2-aminopyridines, and 2-amino benzimidazoles, J. Am. Chem. Soc., 2005; 127: 2211–2217.
15. C.B. Carlson, P.A. Beal, Solid-phase synthesis of acridine based threading intercalator peptides, Bioorg. Med. Chem. Lett., 2000; 10: 1979–1982.

16. A.M. Dar, Shamsuzzaman, S. Tabassum, M. Zakia, A. Sohail, M.A. Gatoo, DNA binding, docking studies, artificial nuclease activity and in vitro cytotoxicity of newly synthesized steroidal1H-pyrimidines, C. R. Chim., 2014; 1045: 62–71.
17. V.A. Bacherikov, J.-Y. Chang, Y.-W. Lin, C.-H. Chen, W.-Y. Pan, H. Dong, R.-Z. Lee, T.-C. Chou, T.-L. Su, Synthesis and antitumor activity of 5-(9-acridinylamino) anisidine derivatives, Bioorg. Med. Chem., 2005; 23: 6513–6520.
18. J. Blasiak, E. Gloc, J. Drzewoski, K.Wozniak, M. Zadrozny, T. Skorski, T. Pertynski, Free radical scavangers can differentially modulate the genotoxicity of amasacrinein normal and cancer cells, Mutat. Res., 2003; 535: 25–34.
19. L. Janovec, M. Kozurkova, D. Sabolova, J. Ungvarsky, H. Paulikova, J. Plsikova, Z. Vantosa, J. Imrich, Cytotoxic 3, 6-bis((imidazolidionone)imino)acridines: synthesis, DNA binding and molecular modelling, Bioorg. Med. Chem., 2011; 19: 1790–1801.
20. Y. Pommier, Drugging topoisomerases: lessons and challenges, ACS Chem. Biol., 2013; 8: 82–95.
21. (a) A.M. Dar, B. Rah, S. Mir, R. Nabi, Shamsuzzaman, M.A. Gatoo, A. Mashrai, Y. Khan, Int. J. Biol. Macromol, 2018; 111: 52–61. (b) A.M. Dar, Shamsuzzaman, M. A. Gatoo, Steroids, 2015; 104: 163–175. (c) A.M. Dar, Shamsuzzaman, M.S. Ahmad, Y. Khan, Med. Chem. Res., 2017; 26: 372–383. (d) A.M. Dar, M.A. Gatoo, A. Ahmad, M.S. Ahmad, M.H. Najar, Shamsuzzaman, J Fluoresc, 2015; 25: 1377–1387.
22. G.S. Son, Binding mode of norfloxacin to calf thymus DNA, J. Am. Chem. Soc., 1998; 120: 6451–6457.
23. Yadav P, Kumar P, Dar AM (2021). Sulfonyl thiosemicarbazones: synthesis, characterization and antibacterial activity. T Appl. Biol. Chem. J; 2(2): 22-26. https://doi.org/10.52679/tabcj.2021.0005
24. M.E. Reicmann, S.A. Rice, C.A. Thomas, P. Doty, A further examination of the molecular weight and size of deoxy pentose nucleic acid, J. Am. Chem. Soc., 1954; 76: 3047–3053.
25. Ayaz Mahmood Dar, Shafia Mir, Masrat Jan, Rizwan Nabi, Manzoor Ahmad Gatoo, Shamsuzzaman. Computational Toxicology, 2021; 17: 100145.
26. D. Mustard, D.W. Ritchie, Docking essential dynamics eigen structures, Proteins: Struct., Funct., Bioinf, 2005; 60: 269–274.
27. T. Mosmann, Rapid colorimetric assay for cellular growth and survival: application to proliferation and cytotoxicity assays, J. Immunol. Methods, 1983; 65: 55–63.
28. N. Shahabadi, S. Kashanian, M. Khosravi, M.Mahdavi, Multispectroscopic DNA interaction studies of a water-soluble nickel(II) complex containing different dinitrogen aromatic ligands, Transit. Met. Chem., 2010; 35: 699–705.
29. A.J. Berk, TBP-like factors come into focous, Cell, 2000; 103: 5–8.
30. A. Wolfe, G.H. Shimer, T. Meehan, A. Wolfe, G.H. Shimer, T. Meehan, Polycyclic aromatic hydrocarbons physically intercalate into duplex regions of denatured DNA, Biochemistry, 1987; 26: 6392–6396.
31. L.F. Tan, H. Chao, K.C. Zhen, J.J. Fei, F. Wang, Y.F. Zhou, L.N. Ji, Effects of the ancillary ligands of polypyridyl ruthenium(II) complexes on their DNA binding and photocleavage behaviours, Polyhedron, 2007; 26: 5458–5468.
32. G. Scatchard, The attractions of proteins for small molecules and ions, Ann. N. Y. Acad. Sci., 1949; 51: 660–672.
33. P.U. Maheswari, M. Palaniandavar, DNA binding and cleavage properties of certain tetrammine ruthenium (II) complexes of modified 1,10-phenonthrolines-effect of hydrogen bonding on DNA-binding affinity, J. Inorg. Biochem, 2004; 98: 219–230.
34. D.L. Pitrak, H.C. Tsai, K. M. Mullane, S. H. Sutton, P. J. Stevens Accelerated neutrophil apoptosis in the acquired immunodeficiency syndrome. Clin Investig, 1996; 98: 2714–2719.